Research Square

Preprints are preliminary reports that have not undergone peer review.
They should not be considered conclusive, used to inform clinical practice,
or referenced by the media as validated information.

Sea-level rise forces global landward expansion of mangroves

Romain Walcker

romain.walcker@univ-tlse3.fr

Université de Toulouse https://orcid.org/0000-0002-5769-810X

François Fromard

CNRS

Biological Sciences - Article

Keywords:

Posted Date: November 27th, 2026

DOI: https://doi.org/10.21203/rs.3.rs-11872027/v1

License: This work is licensed under a Creative Commons Attribution 4.0 International License.
Read Full License

Additional Declarations: There is **NO** Competing Interest.

“Sea-level rise forces global landward expansion of mangroves”

Walcker, R. [1*], Fromard, F. [1]

[1] *Université de Toulouse, Toulouse INP, CNRS, IRD, CRBE, Toulouse, France*

[*] Corresponding author

Abstract

Mangroves are widespread tropical ecosystems that thrive along shorelines and coastal rivers. Since the late 2000s, their net global extent are expanding, yet the drivers of this expansion remain unclear in the context of sea-level rise. Analysing four decades of worldwide changes in mangrove extent alongside sea surface heights, we provide a body of evidence that in many regions, rising sea levels have driven a net increase in mangrove cover, primarily through their landward expansion. Globally, sea-level rise pushed mangroves landward by up to ~2,970 m, with ~14,670 km² of landward gains since 1985 (13.7%), vastly outstripping seaward losses (1.7%). Furthermore, we found that short-term climate variability and the post-2010 climate shift modulated the pace of this expansion by temporarily altering local rates. Based on observational data, these findings underscore sea-level rise as a primary catalyst for global mangrove change. Sustaining this new adaptation mechanism will critically depend on preserving unobstructed landward accommodation space in coastal planning.

Main text

Introduction

Occupying nearly 75% of tropical coastlines, mangroves are critical habitats that vitally sustain marine and terrestrial biodiversity while storing substantial amounts of blue carbon (1). These forest ecosystems thrive under severe environmental constraints, characterised by high salinity, cyclic tidal fluctuations, and intense sediment dynamics. Consequently, mangroves have evolved adaptive strategies that fuel their strong colonising capacity and render them remarkably resilient to environmental changes. Historically undervalued and heavily deforested for aquaculture during the 1980s, these ecosystems have increasingly become targets for conservation and restoration, driven by a growing recognition of their socio-ecological value (2, 3). Recently, a satellite-based assessment tracking four decades of global mangrove cover revealed an unexpected net expansion since the late 2000s that reversed historical losses (4). Yet, observational evidence identifying the underlying drivers of this expansion remains scarce, particularly regarding the influence of sea-level rise. Bridging this knowledge gap is crucial for aligning conservation strategies with new ecosystem trajectories and sustaining long-term recovery under accelerating climate change (5).

Sea-level rise is the most prominent manifestation of climate change for coastal ecosystems worldwide (6−8). It has steadily accelerated in recent years, driven by ocean

thermal expansion and land-ice melt (9, 10). Across global mangrove habitats, sea level rose at an average rate of 3.4±0.9 mm yr^{-1} over the 1985–2025 period. Following 2010, an acceleration phase pushed the global mean to 4.5±1.4 mm yr^{-1}, with the upper quartile reaching 5.3 mm yr^{-1}, while some local rates doubled pre-2010 values to peak at 10.8 mm yr^{-1} in the Caribbean **(**Fig. 1a). Interannual climate variability, including sea-surface height anomalies driven by the El Niño–Southern Oscillation (ENSO), superimposed on these long-term trends, inducing short-term fluctuations exceeding 30 to 50 cm during extreme events (11). Furthermore, in deltaic environments, natural and human-induced land subsidence have amplified these overall rates (12).

Much like salt marshes, tidal flats, and seagrass meadows, mangroves occupy low-gradient intertidal zones where minor shifts in sea level exert profound ecological impacts (8). Long recognised as a threat (6), sea-level rise can imply ecosystem mortality while offering new opportunities for expansion through landward migration into adjacent environments. To examine the extent to which this mechanism have operated globally and contributed to the recent rebound in mangrove extent, we analysed the spatial patterns of annual changes in mangrove cover alongside sea surface heights over the past four decades. To ensure our analysis identified environmental forcing rather than direct human activities, we focused exclusively on pristine areas free from aquaculture, restoration, saltpans, dikes, and urban encroachment (see Methods).

Mangroves prove resilient despite critical rates of sea-level rise

Sedimentary archives reveals how mangroves adjusted to rapid post-glacial sea-level rise, long before sea levels peaked during the mid-Holocene highstand (13). In wave-sheltered, low-energy settings, mangrove stands adapted by growing vertically to prevent drowning. Their dense root systems trapped suspended sediment to build soil elevation, thereby sustaining seedling survival. However, biological and physical thresholds constrained this adaptive capacity, beyond which stands declined (14). Based on these paleo-records, vertical adjustment constraints place the limit for in situ survival between 5 and 8 mm yr^{-1}. Beyond such limits, prolonged submergence and erosion are expected to affect lower intertidal zones, ultimately drowning seedlings and roots.

Whether contemporary mangroves undergo widespread collapse under rapid current sea-level rise remains a critical question with profound implications for coastal biodiversity and blue carbon management (15, 16). We addressed this issue by focusing on mangroves exposed over the past 15 years to critical rates of sea-level rise, defined here as exceeding 6 mm yr^{-1}. We chose the past 15 years as a reference period because they mark the end of the early-2000s global warming slowdown, during which natural climate variability temporarily dampened anthropogenic sea-level rise (17). Since 2010, critical rates of sea-level rise within the mangrove geographical domain have clustered primarily into two major hotspots: the Caribbean and Gulf of Mexico region, and the western Pacific (purple, Fig. 1a). Across these clusters, mangrove cover expanded by 47.8% since 1985 while losses accounted for only 15.1% (Fig. 1b). Sustained losses, potentially signalling incipient collapse, remained confined to a few localised areas, predominantly in the Caribbean and Gulf of Mexico region (Fig. 1c). In these areas, losses (31.0%) exceeded gains (19.2%), resulting in a net extent loss of 11.9%. Focusing on the region with the greatest decline (Fig. 1d), we found that even where mangrove loss

dominated along the seaward margin (within ±200 m of the shoreline), recent expansion occurred in the back-mangrove zone (>1,000 m inland). Caribbean mangroves are particularly vulnerable to rising sea levels, largely owing to their microtidal regimes and limited sediment supply (18). Moreover, in this basin, sea-level rise compounds the effects of hurricanes (19) and extreme winter freezes (20) to drive ecosystem change. Elsewhere in sea-level rise hotspots, widespread mangrove collapse has yet to occur, suggesting a potential lateral shift of the ecosystem.

Global mangroves migrated landward over recent decades

Sea-level rise can enable mangroves to colonise newly suitable landward habitats beyond their current upper intertidal boundary even in places where loss dominates at the seaward edge (6–8). Mechanistically, rising sea levels drive landward saltwater intrusion and alter inundation hydroperiods, converting higher-elevation coastal marshes, supratidal flats, or lowland freshwater ecosystems into suitable mangrove habitats. This landward expansion critically depends on local topography, requiring sufficient and unobstructed accommodation space to take place (21). Indeed, in many regions, hard engineering structures such as seawalls, dikes, and transport infrastructure impede this accommodation space, effectively halting ecosystem landward migration.

Global mapping demonstrates that many regions experienced mangrove landward migration over the past four decades (Fig. 2). Hotspots of landward migration clustered mainly in northern Australia, West Africa, and the Middle East. In these regions, mangroves migrated upstream along river networks by an average of 138±264 m (interquartile range: 21−162 m), reaching up to 2,972 m in northern Australia (Table 1). At the global scale, landward expansion significantly exceeded seaward losses (Table 2). Landward gains represented 13.7% of the 1985 mangrove cover, whereas seaward losses account for only 1.7%. Our findings therefore contrast with previous global and regional projections suggesting that landward migration will ultimately fail to offset seaward losses, demonstrating instead that global mangroves maintain remarkable resistance by actively colonising newly suitable habitats (7, 8, 21).

Landward expansion stems primarily from the landward shift of the intertidal frame under rising sea levels, though the underlying ecological mechanisms vary across hydroclimatic settings. In humid settings, sea-level rise drove saltwater intrusion into brackish or freshwater zones (Fig. 3a, b). The resulting salinity stress suppressed freshwater vegetation, allowing mangroves to expand by outcompeting less salt-tolerant species (22–26). Conversely, on arid, hypersaline supratidal flats (Fig. 3c, d), enhanced tidal flushing diluted interstitial soil salinity, enabling inland mangrove colonisation (27, 28). Together, these contrasting, climate-dependent salinity dynamics facilitate landward expansion where topography or human barriers do not obstruct progression. Over longer timescales, this sea-level-driven colonisation has fundamentally shaped the carbon storage capacity of coastal wetlands (29, 30). Indeed, long-term reconstructions indicate that rapid early-Holocene sea-level rise initiated landward migration that doubled root-zone organic carbon storage rates by continually creating accommodation space for carbon burial. However, how short-term variability has modulated sea-level-driven expansion in recent years, and whether progression proceeds continuously, requires closer examination.

Climate variability modulated sea-level-driven mangrove changes

Superimposed on mean sea-level rise, natural modes of climate variability have rapidly and temporarily modulated sea surface heights over the past four decades (31). These intrinsic climate patterns alter local sea levels through large-scale wind-driven transport, ocean thermal expansion, and atmospheric pressure anomalies, creating basin-wide seesaw effects (11). Recent work suggests that the trans-Pacific ENSO pendulum partially governs short-term mangrove growth dynamics (32). At the upper intertidal limit of mangrove stands, temporary lowstands caused acute soil desiccation and elevated salinity in regions with a pronounced dry season, driving localized mortality along the landward fringe. Conversely, temporary highstands caused prolonged inundation and mortality, an effect particularly pronounced in microtidal settings where minor water-level surges exceed the narrow vertical tidal range.

We evaluated the relationship between mangrove cover changes and climate-driven sea surface height oscillations using maximum covariance analysis, a widely recognised statistical approach in climatology, oceanography, and geophysics (33). Masked beneath the linear trend of sea-level rise, the first dominant pattern, explaining over half of the remaining cross-covariance, reveals a clear inflection point around 2010 (Fig. 4a). This finding aligns particularly well with recent work identifying this period as the turning point that reversed decades of mangrove loss (4). Indeed, this period marked an inflection after which sea-level rise accelerated under the influence of internal climate variability (10). This shift corresponds to the end of the early-2000s global warming hiatus, driven by large-scale modes including the Pacific Decadal Oscillation (PDO) and a strongly negative North Atlantic Oscillation (NAO) phase. Across the Middle East and southern Indonesia, though more patchily elsewhere, mangroves synchronously accelerated their inland expansion (Fig. 4a). The ENSO seesaw pattern is clearly captured by the second mode of variability, which accounts for 22% of the cross-covariance (Fig. 4b). This mode expresses an opposition between the Western Pacific and the South Pacific and the Caribbean, while exerting a moderate yet significant influence across the Red Sea region. This observation agrees with recent work pointing to the impacts of ENSO on observed massive mangrove diebacks and recovery (34−37). Finally, we detected a third mode, accounting for 10% of the cross-covariance, centred primarily over the Atlantic Ocean and pointing to a potential influence of the NAO (Fig. 4c). In a previous study covering 1950-2010, we demonstrated that mangrove cover variations along the French Guiana coastline (spanning roughly 300 km) were tightly linked to multidecadal wave fluctuations governed by the NAO (38). This result underscores the need to account for additional climate drivers associated with internal climate modes, including wave regimes (39), coastal sediment supply (40), precipitation patterns (41), and temperature anomalies (42). Collectively, these forcings modulate mangrove cover changes, acting as compounding drivers alongside sea-level rise.

Conclusion

Our analysis provides a compelling body of evidence that sea-level rise has shaped mangrove cover changes over the past four decades, acting as the primary driver of landward expansion. Ultimately, this establishes sea-level rise as a major catalyst for global mangrove redistribution—a critical mechanism that requires finer-scale local investigations to better resolve its compound interactions with other climatic drivers. We advocate that ensuring landward accommodation space is critical to enable ecosystem migration, whereas constructing

hard coastal barriers obstructs retreat, escalates financial costs, and amplifies sea-level rise impacts on shoreline stability, as observed along the coast of Guyana (43). The landward expansion of mangroves often occurs at the expense of other ecologically valuable habitats, including agricultural croplands, pastures, salt marshes, and terrestrial forests. Because replacing these adjacent coastal ecosystems does not inherently represent a net ecological gain, management strategies must account for these cross-ecosystem trade-offs and prioritise conservation based on relative ecological functions, biodiversity value, and local livelihood needs.

Tables and figures

Table 1: Landward migration statistics across representative regions. Regional and global estimations of landward mangrove migration (m) and linear sea-level rise trends (mm yr^{-1}), reported as mean ± SD and interquartile range (Q25–Q75) computed over 1985–2025 for pristine mangrove areas.

Region (pristine part)	Landward migration Mean ± SD (m)	Landward migration Q25–Q75 (m)	Landward migration Max (m)	Sea-level rise Mean ± SD (mm/yr)
Northern Australia	335 ± 593	36–300	2972	3.67 ± 0.19
West Africa	769 ± 662	286–981	1824	3.05 ± 0.11
Middle East	147 ± 192	28–193	965	3.14 ± 0.27
Caribbean	108 ± 160	17–134	877	3.55 ± 1.14
New Zealand	79 ± 47	50–88	174	4.59 ± 0.29
Global	138 ± 264	21–162	2972	3.41 ± 0.88

Table 2: Mangrove cover and cumulative landward and seaward gains and losses across biogeographic regions since 1985. Values are reported for pristine regions, with percentage gains expressed relative to 1985 mangrove cover and percentage losses expressed relative to 2025 mangrove cover.

Region (pristine part)	Mangrove cover 1985 (km²)	Mangrove cover 2025 (km²)	Landward gains (km²)	Landward losses (km²)	Seaward gains (km²)	Seaward losses (km²)
Southeast Asia	27,379.6	27,887.9	2826.0 (10.3%)	2411.1 (8.6%)	370.2 (1.4%)	276.7 (1.0%)
South America	18,108.9	18,072.8	2587.8 (14.3%)	2419.7 (13.4%)	432.5 (2.4%)	636.6 (3.5%)
West & Central Africa	14,929	15,453.0	2024.0 (13.6%)	1483.9 (9.6%)	52.2 (0.3%)	68.3 (0.4%)
Australia & New Zealand	9,785.1	11,280.7	1982.1 (20.3%)	590.0 (5.2%)	215.5 (2.2%)	112.0 (1.0%)
Caribbean	6,591.6	6,561.3	1289.0 (19.6%)	1252.5 (19.1%)	183.8 (2.8%)	250.7 (3.8%)
North & Central America	8,751.4	8,742.2	1246.2 (14.2%)	1255.2 (14.4%)	76.3 (0.9%)	76.5 (0.9%)
Eastern & Southern Africa	7,356.9	7,250.7	996.2 (13.5%)	1153.0 (15.9%)	163.8 (2.2%)	113.2 (1.6%)
Pacific Islands	6,553.6	6,907.5	816.7 (12.5%)	486.8 (7.0%)	160.4 (2.4%)	136.4 (2.0%)
South Asia	7,504.3	7,994.6	773.6 (10.3%)	404.9 (5.1%)	376.2 (5.0%)	254.6 (3.2%)
The Middle East	220.8	357.5	129.5 (58.7%)	16.8 (4.7%)	27.9 (12.6%)	4.0 (1.1%)
East Asia	10	10.6	1.3 (12.6%)	0.9 (8.3%)	0.3 (2.6%)	0.0 (0.4%)
Global	107191.1	110,518.8	14672.4 (13.7%)	11474.8 (10.4%)	2059.1 (1.9%)	1929.0 (1.7%)

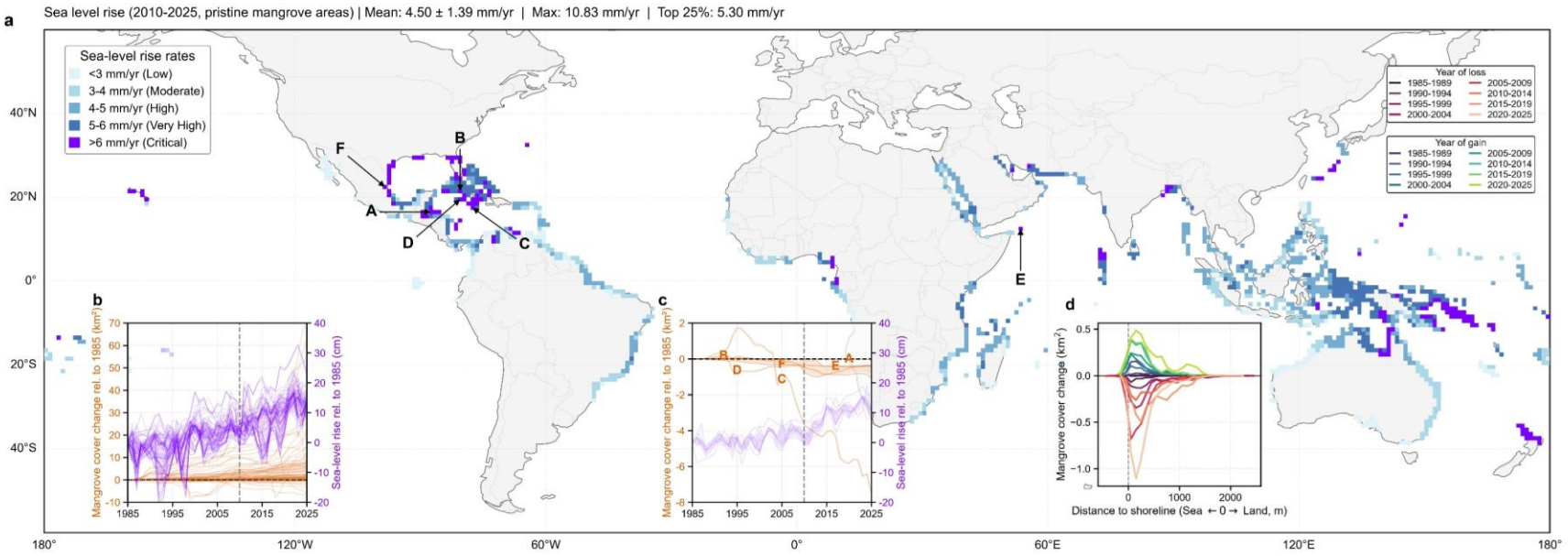


Fig. 1: No widespread mangrove collapse despite critical rates of sea-level rise. a, Global map of sea-level rise rates from 2010 to 2025 across the coastal mangrove domain, classified into five sensitivity bins ranging from low to critical. Letters (A–F) indicate specific coastal areas experiencing persistent mangrove cover decline since 2010. **b**, Temporal evolution of mangrove cover change (amber-orange; median and 25th–75th percentile envelope) and sea-level rise (purple; median and 25th–75th percentile envelope) relative to the 1985 baseline across areas experiencing critical sea-level rise rates since 2010 (vertical dashed line). Low-opacity background lines show individual area trajectories, with nearly all mangroves within these zones exhibiting net area gains. **c**, Time series of mangrove cover change for the six areas exhibiting persistent decline between 2010 and 2025, with individual curves labelled (A–F) to match the locations mapped in a. **d**, d, Cross-shore distribution of mangrove cover changes between 1985 and 2025 across the area experiencing the highest rate of loss since 2010 (letter C). The x-axis shows distance to the 1984 shoreline, with positive values landward and negative values seaward. Colour gradients indicate the year of change, using green shades for gains and red shades for losses.

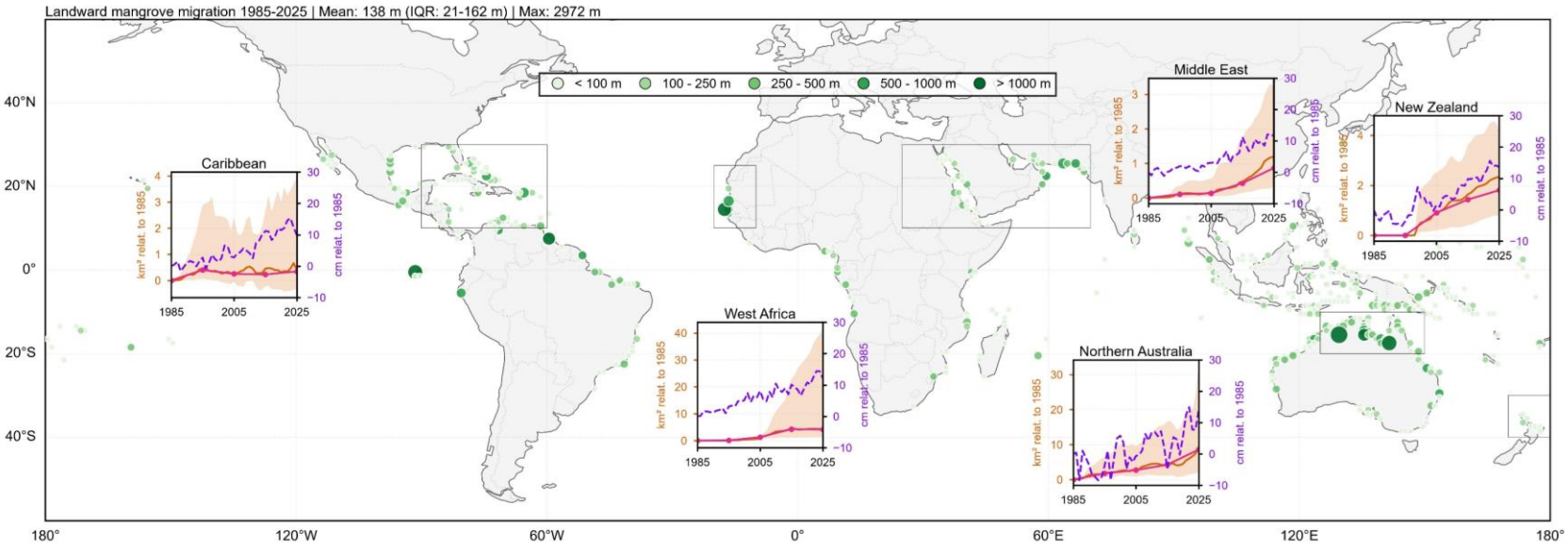


Fig. 2: Global landward migration of mangroves (1985-2025). Global map showing the widespread distribution of mangrove landward migration. Proportional circles denote migration magnitude classified into five categories. Inset panels for key study regions (Caribbean, West Africa, Middle East, Northern Australia, and New Zealand) display regional time series with median and interquartile range envelopes for mangrove area changes relative to the 1985 baseline (solid orange lines, left axes) alongside relative sea-level rise (dashed purple lines, right axes). Landward extent expansion is shown as a pink line on the left axis.

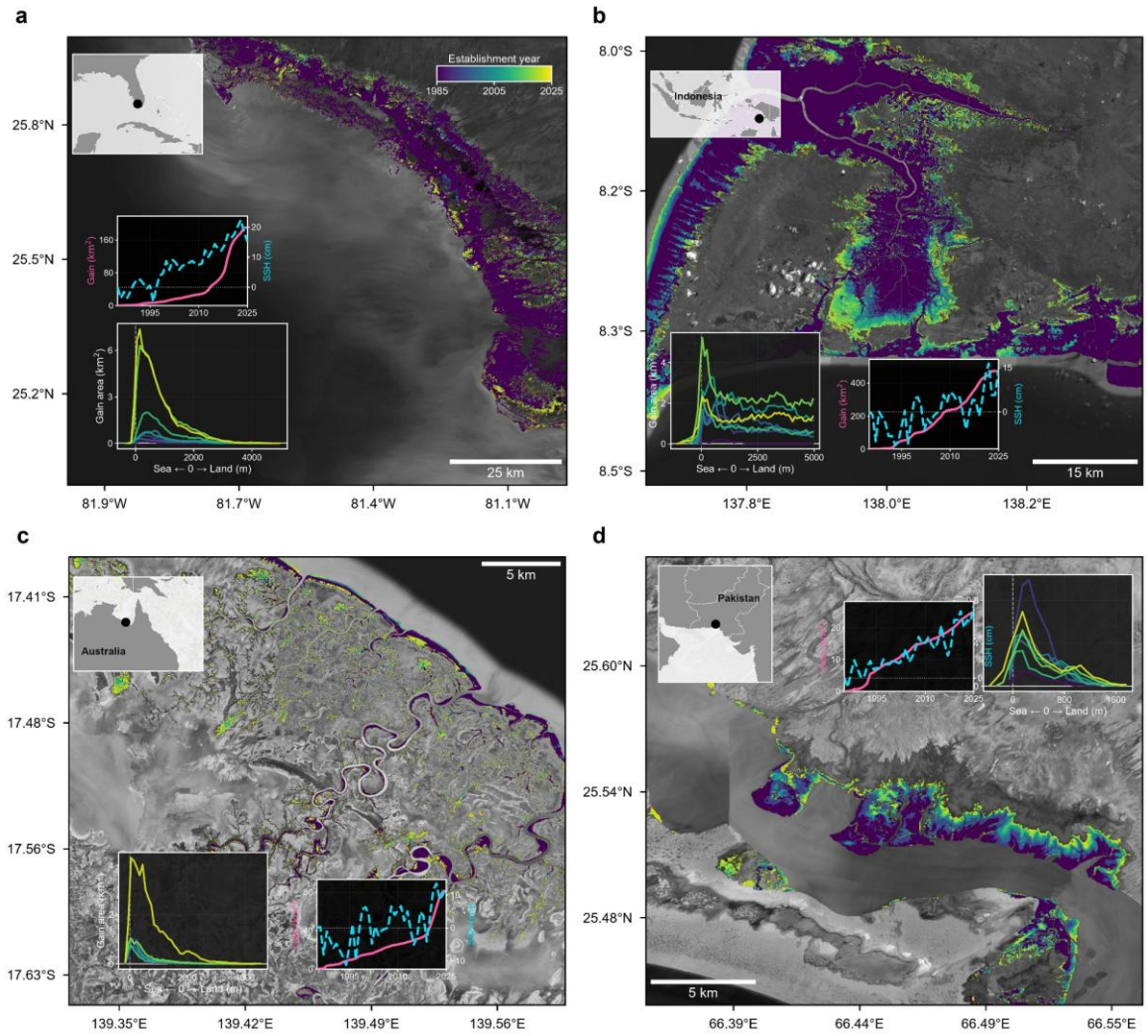


Fig. 3: Landward expansion of mangroves across representative global settings. Maps show mangrove establishment year (1985–2025) overlaid on grayscale Esri World Imagery basemaps for four study sites: **a**, Everglades, USA; **b**, South Papua; **c**, Northern Australia; and **d**, Pakistan Coast. Cross-shore insets show gained mangrove area binned by distance relative to the 1984 reference water baseline, colored by establishment period matching the map palette. Secondary insets show relative changes in sea-surface height (SSH, cm) and mangrove cover area relative to the 1985 baseline.

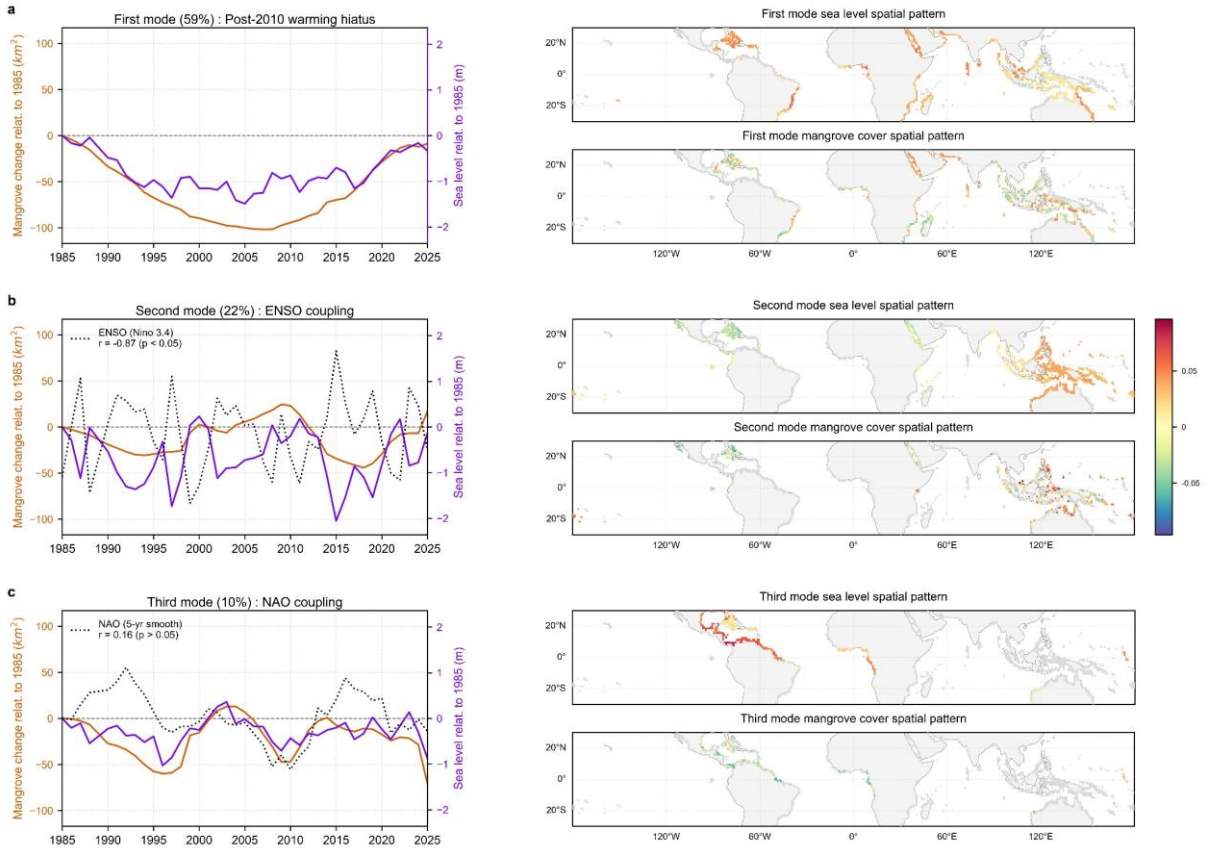


Fig. 4: Climate variability beyond long-term linear trends. a, First Maximum Covariance Analysis (MCA) mode between detrended annual sea-surface height and mangrove cover change, showing temporal principal components alongside spatial loading maps for sea level and mangrove cover. **b**, Second MCA mode highlighting coupling with the El Niño–Southern Oscillation (ENSO; Niño 3.4 index). **c**, Third MCA mode highlighting potential coupling with the North Atlantic Oscillation (NAO). Spatial maps display statistically significant grid cells ($p < 0.05$), with non-significant areas masked in light grey.

Methods

Mangrove cover extent

Annual mangrove cover maps (1985–2025) at 30 m spatial resolution were retrieved from the Global Mangrove Watch repository (GMW v4.1.12; 44). The dataset comprises 1,696 1°×1° tiles, each formatted as a 41-band binary raster where each band corresponds to an annual map. All tiles were reprojected to the World Cylindrical Equal Area projection to calculate annual changes in mangrove extent. To quantify these changes, the area of mangrove cover for each tile and year was derived by multiplying the count of active mangrove pixels (DN = 1) by the specific surface area of a single pixel in the projected coordinate system (~900 m^2) and then converted into square kilometres. To isolate climate-driven dynamics from direct anthropogenic drivers, tiles were manually classified into 'pristine' or 'non-pristine' by visual cross-examination against high-resolution Google Earth satellite imagery. A tile was designated as pristine when its mangrove perimeter showed no evidence of massive aquaculture ponds, saltpans, dikes, or major urban encroachment. Consequently, most tiles across India and Southeast Asia were excluded due to dense aquaculture coverage, while numerous tiles in West Africa were omitted owing to widespread rice cultivation and saltpans. Similarly, in Central Africa, several tiles were discarded due to intense coastal urbanization, and tiles within the Wouri estuary and Niger delta were removed because of oil extraction activities affecting mangroves. This screening retained 1,261 pristine tiles for analysis.

Sea surface height data

Sea surface height data, expressed in meters above the geoid, were retrieved from the European Centre for Medium-Range Weather Forecasts (ECMWF) Ocean Reanalysis System 5 (ORAS5) via the Copernicus Climate Data Store (45). Provided in NetCDF4 format at a 0.25°×0.25° spatial resolution, ORAS5 assimilates global oceanographic observations into ocean models to construct a spatially continuous baseline spanning 1958–2026. By accurately resolving regional sea-level variations and coastal hydrodynamics, ORAS5 offers a robust framework for evaluating climate-driven mangrove dynamics. For each 1°×1° pristine mangrove tile, annual mean sea surface height values were extracted across the 1985–2025 study period. Specifically, tile centroids were computed in WGS84 from the Global Mangrove Watch (GMW v4.1) tile grid, matched to the nearest valid (non-land) ocean grid cell using Euclidean distance, and averaged annually from monthly reanalysis fields.

Calculation of sea-level rise rates

For each mangrove tile, temporal trends in sea-level were evaluated using ordinary least-squares linear regression over two distinct intervals: the long-term historical baseline (1985–2025), and a recent post-2010 period (2010–2025). Annual rates (mm yr^{-1}) were derived from the regression slope of sea surface heights. Summary statistics, including the mean, standard

deviation (reported as mean ± SD), maximum values, and the 75th percentile (top 25% threshold), were computed across all tiles.

Dating mangrove gains and losses

To determine the year of gain for mangroves present in 2025, we traced each 2025 mangrove pixel backward through the 1985–2025 GMW stack to its most recent non-mangrove year. Symmetrically, for pixels ever mapped as mangrove but absent in 2025, we identified their last year of presence as the year of loss.

Gain and loss in areas experiencing critical rates of sea-level rise

To assess mangrove cover changes under high-exposure conditions, tiles were filtered to isolate those experiencing critical rates exceeding 6 mm yr^{-1} during the 2010–2025 period, having a minimum mangrove surface area 0.1 km^2 in 1985, and exhibiting significant net trends > 5%. Within this filtered subset, annual changes in mangrove cover and sea-level were expressed relative to their 1985 baselines. Additionally, a subset of persistently declining tiles was isolated to examine structural collapse, defined as tiles exhibiting a sustained, uninterrupted surface reduction exceeding 5% relative to the 1985 baseline across every single year from 2010 to 2025.

Landward and seaward distances

We retrieved the JRC Global Surface Water Yearly History collection (46) from Google Earth Engine (47) and exported multi-band annual time series at a 100 m resolution for pristine mangrove tiles. From these records, we generated two water and land masks, a historical baseline (1984) and the most recent available baseline (2021), by gap-filling missing observations with subsequent (1984) or prior (2021) valid records and binarizing permanent water against land. To distinguish landward from seaward dynamics, we calculated Euclidean distances from mangrove gain pixels to the historical historical baseline, and from mangrove loss pixels to the recent baseline.

Landward migration

To quantify landward mangrove migration between 1985 and 2025, we computed Euclidean distances from each mangrove pixel to the historical water and land baselines on a tile-by-tile basis at decadal intervals (1985, 1995, 2005, 2015, and 2025). For each tile, we tracked the maximum landward distance of mangrove occurrence, isolated tiles exhibiting net landward displacement, and calculated the cumulative shift as the difference in maximum landward distance between 1985 and 2025.

Coupling patterns with climate variability

To isolate dominant modes of coupled variability between mangrove cover and sea surface height, we performed maximum covariance analysis via singular value decomposition.

Prior to analysis, time series for both fields were linearly detrended point-by-point and standardized. This detrending removed secular background trajectories—such as continuous global sea level rise—thereby isolating interannual-to-decadal covariability driven by climate oscillations rather than long-term trends. Singular value decomposition factorizes the cross-covariance matrix of the standardized fields into orthogonal modes, each quantifying a specific fraction of squared covariance. Each mode yields paired spatial anomaly maps and corresponding temporal expansion coefficients that capture shared spatio-temporal dynamics. Finally, relationships between fields were evaluated using Pearson correlation coefficients (r) and coefficients of determination (r^2), with statistical significance determined at $p < 0.05$.

Data availability

All raw input datasets used in this study are publicly available from their original repositories as described in the Methods section. Precomputed intermediate spatial and tabular datasets are archived on Zenodo (https://doi.org/10.5281/zenodo.24526648) under a Creative Commons Attribution 4.0 International (CC-BY 4.0) license. The Zenodo record is currently restricted during peer review and will be made publicly accessible upon manuscript acceptance.

Code availability

All Jupyter notebooks and documentation used for data formatting, spatial processing, distance calculations, and figure generation are available on GitHub at https://github.com/WalckR/Mangroves_and_sea-level_rise under the MIT License.

References

1. Lee, S. Y. *et al.* Ecological role and services of tropical mangrove ecosystems: a reassessment. *Global Ecology and Biogeography* **23**, 726–743 (2014).
2. Duke, N. C. *et al.* A world without mangroves? *Science* **317**, 41–42 (2007).
3. Friess, D. A. *et al.* Mangroves give cause for conservation optimism. *Current Biology* **30**, R153–R154 (2020).
4. Zhang, Z. *et al.* Unexpected expansion and regrowth in Earth's mangrove forests over the past four decades. *Science* **392**, 1082–1087 (2026).
5. Heller, N. E., & Zavaleta, E. S. Biodiversity management in the face of climate change: a review of 22 years of recommendations. *Biological Conservation*, 142, 14–32 (2009).
6. Gilman, E. L. *et al*. Threats to mangroves from climate change and adaptation options: A review. *Aquatic Botany* **89**, 237–250 (2008).
7. Lovelock, C., Cahoon, D., Friess, D. *et al.* The vulnerability of Indo-Pacific mangrove forests to sea-level rise. *Nature* **526**, 559–563 (2015).
8. Osland, M. J. *et al.* Migration and transformation of coastal wetlands in response to rising seas. *Science Advances* **8**, eabo5174 (2022).
9. Nerem, R. S. et al. Climate-change–driven accelerated sea-level rise detected in the altimeter era. Proc. *Natl. Acad. Sci. U.S.A.* **115**, 2022–2025 (2018).
10. Leclercq, L. et al. Abrupt trend change in global mean sea level and its components in the early 2010s. *Commun. Earth Environ.* **7**, 130 (2026).
11. Widlansky, M. J. *et al.* Future extreme sea level seesaws in the tropical Pacific. *Sci. Adv.* **1**, e1500560 (2015).
12. Nicholls, R. J. *et al.* A global analysis of subsidence, sea-level rise and coastal adaptation needs. *Nature Climate Change* **11**, 338–342 (2021).
13. Saintilan, N. *et al.* Thresholds of mangrove survival under rapid sea-level rise. *Science* **368**, 1118–1121 (2020).
14. Saintilan, N. *et al.* Widespread retreat of coastal habitat is likely at warming levels above 1.5° C. *Natur*e **621**, 112–119 (2023).
15. Nagelkerken, I. *et al.* The habitat function of mangroves for terrestrial and marine fauna: A review. *Aquatic Botany* **89**, 155–185 (2008).
16. Donato, D. *et al.* Mangroves among the most carbon-rich forests in the tropics. *Nature Geosci* **4**, 293–297 (2011).
17. Cazenave, A. *et al.* The rate of sea-level rise during the warming hiatus. *Nature Climate Change* **4**, 358–361 (2014).
18. Woodroffe, C.D. *et al.* Mangrove Sedimentation and Response to Relative Sea-Level Rise. *Annual Review of Marine Science* **8**, 243–266 2016.
19. Krauss, K. W. & Osland, M. J. Tropical cyclones and the organization of mangrove forests: a review. *Annals of Botany* **125**, 213–234 (2020).
20. Kang, Y. *et al.* Mangrove freeze resistance and resilience across a tropical-temperate transitional zone. *Journal of Ecology* **113**, 94–111 (2025).
21. Schuerch, M. *et al.* Future response of global coastal wetlands to sea-level rise. *Nature* **561**, 231–234 (2018).
22. Saha A. K. *et al*., Sea level rise and South Florida coastal forests. *Climatic Change* **107**, 81–108 (2011).
23. Krauss, K.W. *et al.* Sea-level rise and landscape change influence mangrove encroachment onto marsh in the Ten Thousand Islands region of Florida, USA. *J. Coast Conserv.* **15**, 629– 638 (2011).

24. Chimner, R.A. *et al.* Current extent and historical expansion of introduced mangroves on Oahu Hawaii. *Pac Sci.* **60**, 377–383 (2006).
25. Smith, T.J. *et al.* Dynamics of Mangrove-Marsh Ecotones in Subtropical Coastal Wetlands: Fire, Sea-Level Rise, and Water Levels. *fire ecol* **9**, 66–77 (2013).
26. Perry, C.L. & Mendelssohn, I.A. Ecosystem effects of expanding populations of *Avicennia germinans* in a Louisiana salt marsh. *Wetlands* **29,** 396–406 (2009).
27. López-Medellín X. *et al.,* Oceanographic anomalies and sea-level rise drive mangroves inland in the Pacific coast of Mexico. *J. Veg. Sci.*, **22**, 143–151 (2011).
28. Etemadi, H. *et al.* Forest migration and carbon sources to Iranian mangrove soils. *Journal of Arid Environments* **157**, 57–65 (2018).
29. Rogers K. *et al*., Wetland carbon storage controlled by millennial-scale variation in relative sea-level rise. *Nature* **567**, 91–95 (2019).
30. Lovelock, C. & Reef, R. Variable Impacts of Climate Change on Blue Carbon. *One Earth* **3**, 195–211 (2020).
31. Stammer, D. *et al.* Causes for Contemporary Regional Sea Level Changes. *Annu. Rev. Mar. Sci.* **5**, 21–46 (2013).
32. Zhang, Z. *et al.* Global mangrove growth variability driven by climatic oscillation-induced sea-level fluctuations. *Nature Geoscience* **18**, 488–494 (2025).
33. Bretherton, C. S. *et al.* An intercomparison of methods for finding coupled patterns in climate data. *Journal of Climate* **5**, 541–560 (1992).
34. Duke, N. C. *et al*., ENSO-driven extreme oscillations in mean sea level destabilise critical shoreline mangroves—An emerging threat. *PLOS Clim.* **1**, e0000037 (2022).
35. Lovelock, C. E. *et al.* Mangrove dieback during fluctuating sea levels. *Sci Rep* **7**, 1680 (2017).
36. Ahmed, M.M., Awaleh, M.O., Ibrahim, A.Y. et al. Long term mangrove dieback and recovery at Godorya Marine Protected Area in the Gulf of Aden under climate variability. Sci Rep 16, 19275 (2026).
37. L. Carruthers *et al.*, Sea-level rise and extreme Indian Ocean Dipole explain mangrove dieback in the Maldives. *Sci. Rep.* **14**, 27012 (2024).
38. Walcker R. *et al.* Fluctuations in the extent of mangroves driven by multi-decadal changes in North Atlantic waves. *Journal of Biogeography* **42**, 2209–2219 (2015).
39. Wells, S. *et al.* Global mangrove distribution on the open coast is controlled by waves. *Nature* (2026).
40. Balke, T. *et al.* Windows of opportunity: thresholds to mangrove seedling establishment on tidal flats. *Marine Ecology Progress Series* **440**, 1–9 (2011).
41. Eslami-Andargoli, L. *et al.* Mangrove expansion and rainfall patterns in Moreton Bay, Southeast Queensland, Australia. *Estuar. Coast. Shelf Sci.* **85**, 292–298 (2009).
42. Cavanaugh K. C. *et al.* Poleward expansion of mangroves is a threshold response to decreased frequency of extreme cold events. *Proc. Natl. Acad. Sci. U.S.A.* **111**, 723–727 (2013).
43. Anthony, E. J. *et al.* Coastal engineering and large-scale mangrove destruction in Guyana, South America: Averting an environmental catastrophe in the making. *Ecol. Eng.* **47**, 268–273.
44. Bunting, P. *et al.* Global Mangrove Watch: Timeseries of Mangrove Extent (Version 4.1.12). *Zenodo* https://doi.org/10.5281/zenodo.21346457 (2026).
45. Copernicus Climate Change Service. ORAS5 global ocean reanalysis monthly data from 1958 to present. *Copernicus Climate Change Service Climate Data Store* https://doi.org/10.24381/cds.67e8eeb7 (2021).
46. Pekel, J-F *et al.* High-resolution mapping of global surface water and its long-term changes. *Nature* **540**, 418–422 (2016).

47. Gorelick, N. *et al.* Google Earth Engine: Planetary-scale geospatial analysis for everyone. *Remote Sens. Environ.* **202**, 18–27 (2017).